



1 An Efficient Algorithm for Improved Doppler Profile 2 Detection of MST Radar Signals

3 Nimmagadda Padmaja¹, Souri Varadarajan², Polisetti Yashoda³ Enugonda Ramyakrishna⁴

4 ¹Professor, Department of Electronics and Communication Engineering, Sree Vidyanikethan Engineering
5 College, Tirupati, Andhra Pradesh, India-517102.

6 ²Professor, Department of ECE, S V University College of Engineering, Tirupati, Andhra Pradesh, India.

7 ³Scientist D, National Atmospheric Research Laboratory, Indian Space Research Organization, AP, India.

8 ⁴Junior Research Fellow (ISRO Project), Sree Vidyanikethan Engineering College, Tirupati, AP, India.

9 *Correspondence to:* N.Padmaja (padmaja202@gmail.com)

10 **Abstract:** An efficient algorithm based on Empirical Mode Decomposition (EMD) de-noising using soft
11 threshold techniques for accurate doppler profile detection and Signal to Noise Ratio (SNR) improvement of
12 MST Radar Signals is discussed in this paper. Hilbert Huang Transform (HHT) is a time-frequency analysis
13 technique for processing radar echoes which constitutes EMD process that decomposes the non-stationary
14 signals into Intrinsic Mode Functions (IMFs). HHT process has been applied on the time series data of MST
15 (Mesosphere-Stratosphere-Troposphere) radar collected from NARL (National Atmospheric research
16 Laboratory), Gadanki, India. Further, spectral moments were estimated and signal parameters such as mean
17 doppler, signal power, noise power and SNR were calculated. Stacked doppler profile was plotted to observe the
18 improvement in doppler detection. It has been observed that there is a considerable improvement in recognition
19 of the doppler echo leading to improved Signal Power and SNR. The algorithm was tested for its efficacy on
20 various data sets for all the 6 beams and the results of two data sets are presented.

21 **Keywords:** MST Radar, Empirical Mode Decomposition, De-noising, Hilbert Huang Transform, Doppler, SNR

22 1. Introduction

23 Processing and analysis of radar echoes from MST region pose serious challenges to traditional signal
24 processing techniques especially at higher altitudes above 15 Kms since the echo returns are very weak and
25 buried in noise. The most common approach for analysis of atmospheric radar signals is the Fast Fourier
26 Transform (FFT) and Wavelets. However, Fourier Transforms are not suitable for applications that involve
27 nonlinear and non stationary signals as it has a serious drawback that in transforming to the frequency domain,
28 time information is hidden and not explicitly visible. Wavelet Transform analysis, which is widely used method,
29 overcomes some of the above limitations but there is a need for a-priori knowledge about the kind of scale
30 elements present in the signals and the choice of a suitable mother wavelet for analysis since the accuracy of the
31 results depends on the selection of the wavelet. Hence, an adaptive signal processing technique based on the
32 Empirical Mode Decomposition (EMD) and de-noising using soft thresholding is proposed in this work.

33 2. Indian MST Radar System

34 The MST Radar facility at Gadanki (13.5° N, 79.2° E, 6.3° N mag.lat) is an excellent system used for
35 atmospheric probing in the regions of Mesosphere, Stratosphere and Troposphere (MST) covering up to a height
36 of about 100 km. It is used for coherent backscatter study of the ionospheric irregularities above 100 Km. MST
37 radar is a state-of-the-art instrument capable of providing estimates of atmospheric parameters with very high



38 resolution on a continuous basis which contribute to study different dynamic process in the atmosphere. It is an
39 important research tool in the investigation of prevailing winds, waves, turbulence and atmospheric stability and
40 other phenomenon. The Indian MST radar is highly sensitive, pulse-coded, coherent VHF phased array radar
41 operating at 53 MHz with a peak power-aperture product of $3 \times 10^{10} \text{ Wm}^2$.

42 3. Hilbert Huang Transform

43 Hilbert Huang Transform (HHT) is one of the best time-frequency analysis technique for processing radar
44 echoes. HHT basically comprises Empirical Mode Decomposition process based on numerical shifting to
45 decompose the non-stationary signal into Intrinsic Mode Functions and obtain instantaneous frequency solution.
46 To obtain instantaneous frequency data, Hilbert Spectral Analysis (HSA) method is applied to the IMFs. Since
47 the signal is decomposed in time domain and the IMFs length is the same as the original signal. HHT preserves
48 the characteristics of the varying frequency. Also the, extraction of IMFs enables various de-noising techniques
49 to be applied for accurate detection of doppler echo. This is the key benefit of HHT. It has been tested and
50 validated comprehensively, but only empirically. In all cases studied, from any of the traditional analysis
51 methods, HHT (Padmaja et al., 2011; Jing-tian et al., 2007) gave much sharper results in time-frequency-energy
52 representations. HHT process was applied on time series MST radar data and was investigated for its efficacy.
53 The spectral moments were estimated and signal parameters such as mean doppler, signal power, noise power
54 and SNR were calculated.

55 3.1 Empirical Mode Decomposition

56 The Empirical Mode Decomposition is an effective de-noising technique (Flandrin et al., 2004; Padmaja et al.,
57 2017) that can be used to process non-linear and non-stationary data. This method is adaptive and intuitive. Each
58 oscillatory mode is represented by an IMF that satisfies the conditions of an IMF (Huang et al., 2005). An IMF
59 represents a simple oscillatory mode and it is a counterpart to the simple harmonic function, but it is much
60 general instead of constant amplitude and frequency, as in a simple harmonic component. IMF can have a
61 variable frequency and amplitude as function of time.

62 3.1.1 EMD Algorithm

63 Given a non-stationary signal $x(t)$, the EMD algorithm (Rilling et al., 2003) can be summarized as follows:

- 64 a) Find the local maxima and minima of the signal, then connect all the maxima and minima of signal
65 $X(t)$ and obtain the upper envelope $X_u(t)$ and the lower envelope $X_l(t)$ respectively.
- 66 b) Compute the local mean value $m_1(t) = (X_u(t) + X_l(t))/2$ of data $X(t)$, subtract the mean value from signal
67 $X(t)$ and get the difference: $h_1(t) = X(t) - m_1(t)$.
- 68 c) Assume $h_1(t)$ as new data and repeat steps(1) and (2) for k times, $h_{1k}(t) = h_1(k-1)(t) - m_{1k}(t)$, where $m_{1k}(t)$
69 is the mean value of $h_1(k-1)(t)$ and $h_{1k}(t)$. Step(c) is terminated until the resulting data satisfies the two
70 conditions of an IMF, defined as $c_1(t) = h_{1k}(t)$. The residual data $r_1(t)$ is expressed as $r_1(t) = X(t) - c_1(t)$.
- 71 d) Assume $r_1(t)$ as new data and repeat steps (a-c) and extract all the IMFs. Terminate the sifting process
72 until n^{th} residue $r_n(t)$ becomes less than a predetermined number or the residue becomes monotonic.



73 e) Repeat steps (a-d) till the residual no longer contains any useful frequency information. The original
 74 signal is equal to the sum of its IMFs. If we have ‘n’ IMFs and a final residual $r_n(t)$, the original signal
 75 $X(t)$ can be defined as follows

76
$$X(t) = \sum_{i=1}^n c_i + r_n \quad \text{----- (1)}$$

77 **3.2 Intrinsic Mode Functions**

78 After the application of EMD (George Tsolis et al., 2011; Flandrin et al., 2004; Norden et al., 1998; Wu et al.,
 79 2004; Dejie Yu et al., 2010), if the residue, r_1 still contains information of longer period components, then it is
 80 again treated as new data and subjected to the sifting process. The sifting process can be stopped by any of the
 81 predetermined criteria: either when the component value c_n or the residue r_n becomes less than the
 82 predetermined value or also when the residue, r_n becomes a monotonic function from which no more IMFs can
 83 be extracted. The criterion for stopping the sifting process is based on limiting the size of the Standard
 84 Deviation (SD), which can be computed from the two consecutive sifting results as shown in the equation (2).

85
$$SD = \sum_{t=0}^T \frac{|h1(k-1)(t) - h1k(t)|^2}{h1^2(k-1)(t)} \quad \text{----- (2)}$$

86 A typical value for SD is around 0.21 to 0.3. Hard and soft thresholding (similar to de-noising in Wavelets) is
 87 used to treat Intrinsic Mode Functions to achieve high SNR.

88 **4. Denoising**

89 Signal de-noising scheme based a multiresolution approach is referred to as empirical mode decomposition de-
 90 noising (Padmaja et al., 2017; Donoho et al, 1995). A smooth version of the input signal can be obtained by
 91 thresholding the IMFs before signal reconstruction. Thresholding are of two types namely Hard and Soft
 92 Threshold. If $\Gamma[\tau_j]$ is a thresholding function, and τ_j is the threshold parameter, the threshold can be determined
 93 in different ways. Donoho and Johnstone proposed a universal threshold, τ_j for removing noise (Donoho et al,
 94 1995). The method of soft threshold is applied to process the radar data. After extracting the Intrinsic Mode
 95 functions in each range bin, de-noising techniques are employed before reconstruction of the Doppler spectra by
 96 using threshold levels.

97 **4.1 Hard Threshold**

98 Hard threshold removes the corresponding IMFs depending on the frequencies if τ_j is less than or equal to 1. The
 99 condition for hard threshold as shown in equation (3) and (4)

100
$$f_j(t) = \text{IMF}_j(t) \quad \text{If } |\text{IMF}_j(t)| > \tau_j$$

 101
$$\text{If } |\text{IMF}_j(t)| \leq \tau_j \quad \text{-----(3)}$$

102
$$f_j(t) = \text{IMF}_j(t) \quad \text{If } |\text{IMF}_j(t)| > \tau_j$$

 103
$$\text{If } |\text{IMF}_j(t)| \leq \tau_j \quad \text{-----(4)}$$

104 **4.2 Soft Thresholding**

105 Soft thresholding process tends to shrink noise towards zero. By taking the median values of IMFs, $\tilde{\sigma}_j$ and τ_j
 106 were calculated using equations (5), (6), and (7).

107
$$\tau_j = \tilde{\sigma}_j \sqrt{2 \cdot \log_e(N)} \quad \text{-----(5)}$$



108 $\sigma_j = \text{MAD}_j / 0.6745$ -----(6)

109 $\text{MAD}_j = \text{Median} \{ |\text{IMF}_j(t) - \text{Median} \{ \text{IMF}_j(t) \}| \}$ -----(7)

110 Where σ_j is the estimation of the noise level of the j^{th} IMF (scale level) and MAD_j represents the absolute
 111 median deviation of the j^{th} IMF. The soft thresholding shrinks the IMF samples by τ_j towards zero as follows.

112 $\hat{f}_j(t) = \text{IMF}_j(t) - \tau_j$ If $\text{IMF}_j(t) \geq \tau_j$
 113 0 If $|\text{IMF}_j(t)| < \tau_j$
 114 $\text{IMF}_j(t) + \tau_j$ If $\text{IMF}_j(t) \leq -\tau_j$ -----(8)

115 The signal can be reconstructed by adding all the IMFs which gives the de-noised signal. This procedure is
 116 applied for all the range bins. The processing steps are discussed in 4.21.

117 **4.2.1 Processing steps for the Algorithm**

- 118 (i) Read the time series data (in '.r' format).
 119 (ii) Convert the .r file into .mat file and read the data from .mat file.
 120 (iii) Calculate IMFs by using EMD method for each range bin and apply Hilbert Transform on each IMF .
 121 (iv) Apply Soft Threshold technique of de-noising as mentioned below.
- 122 • Calculate the noise level of the IMF viz. σ_j (Donoho et al, 1995) by finding the median values
 123 of the IMFs.
 - 124 • Calculate the value of universal Threshold (τ_j) by using the calculated value σ_j .
 - 125 • Taking universal Threshold as reference and the conditions proposed by Donoho and Johnstone,
 126 soft thresholding was done for each range bin.
 - 127 • If the value of IMF is greater than or equal to τ_j , the IMF will be subtracted by τ_j . If the value of
 128 IMF is less than τ_j then IMF value is made zero and if the value of IMF is less than or equal to $-\tau_j$
 129 , then the IMF will be incremented by τ_j ..
 - 130 • This process is applied on all the range bins.
- 131 (v) Reconstruct the signal by adding all the IMFs for each range bin and apply three point running
 132 average method to each range bin.
- 133 (vi) Calculate the mean noise level for each range bin. (Hildebrand et al., 1974).
 134 (vii) Subtract the mean noise level for each range bin and plot the stacked doppler spectrum.
 135 (viii) Calculate the spectral moments viz., Total power (Zeroth moment), Doppler shift (First moment),
 136 Spectral width (Second moment)

137 **5. Moments Calculations**

138 Three lower order Spectral moments (zero, first and second) and SNR are calculated by using adaptive
 139 moments method (Anandan et al., 2004). These three spectral moment represents the signal strength (power),
 140 the weighted mean doppler shift and width of the spectrum (Woodman et al., 1985; Morse et al., 2002; Anandan
 141 et al., 2004). The moments were calculated for the data of 24th July 2002 and 22nd Jan 2007 data by using FFT
 142 and HHT. The expressions for the first three moments are as follows.
 143 The 0th moment representing the total signal power is

144 $M_0 = \sum_{i=m}^n P_i$ -----(9)



145 The 1st moment representing the weighted mean Doppler shift is

146
$$M_1 = (1/M_0) \sum_{i=m}^n P_i f_i \text{ -----(10)}$$

147 The 2nd moment representing the variance, a measure of dispersion from the mean frequency is

148
$$M_2 = (1/M_0) \sum_{i=m}^n P_i (f_i - M_1)^2 \text{ -----(11)}$$

150 Where m, n are the lower and upper limits of the Doppler bin of the spectral window. P_i, f_i are the powers and
 151 frequencies corresponding to the Doppler bins within the spectral window.

152 Signal-to-noise ratio (SNR) in dB is calculated by equation (12).

153
$$\text{SNR} = 10 \log \left(\frac{M_0}{N.L} \right) \text{ -----(12)}$$

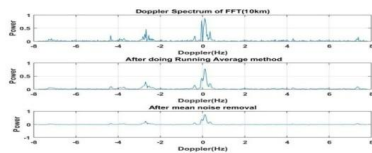
154 Where N and L are the total number of Doppler bins and mean noise level respectively which on multiplication
 155 gives the total noise over the whole bandwidth.

156 Doppler width, which is taken to be the full width of the Doppler spectrum is calculated as:

157
$$\text{Doppler Width} = 2\sqrt{M_2} \text{ -----(13)}$$

158 **6.Results And Discussion**

159 The developed HHT algorithm was applied on various range bins of time series MST Radar data upto 25 Kms.
 160 The corresponding plots for different range bins are shown in figures 1-6. It can be observed that developed
 161 algorithm is able to identify the true peaks of the echo signal. The corresponding Mean Doppler profile plots
 162 using both HHT and FFT are plotted in figures (7a) and (7b). Spectral moments for East beam of 24th July 2002
 163 and 22nd Jan 2007 data using FFT and HHT are plotted in figures 7a-8f. The average values of SNR, Power and
 164 Noise for independent beams of two different data sets are tabulated in Table1. The average values of SNR,
 165 Power and Noise for all the beams are tabulated in Table 2. It is clearly visible from the results that using the
 166 proposed algorithm, the genuine doppler is detected accurately and also there is an improvement of 5.6587 dB in
 167 SNR for 24 July 2002 data and 4.5667 dB improvement of SNR for 22 Jan 2007 data.



168
 169 Figure 1:Doppler spectrum using FFT of height 10km

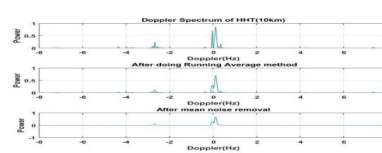
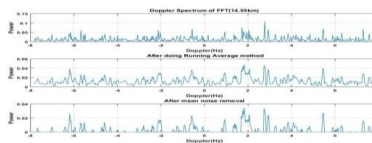


Figure 2:Doppler spectrum using HHT of height 10km



170
 171 Figure 3:Doppler spectrum using FFT of height 14.55km

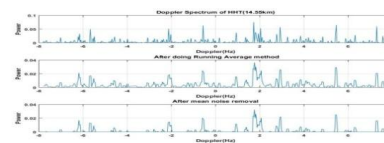
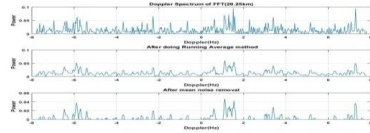


Figure 4:Doppler spectrum using HHT of height 19.5km



172



173

Figure 5: Doppler spectrum using FFT of height 20.25km

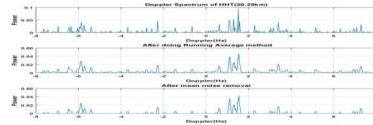
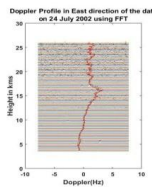
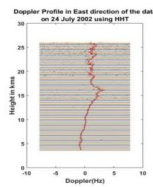


Figure 6: Doppler spectrum using HHT of height 20.25km

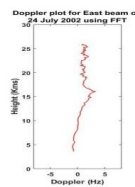
174



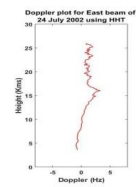
Fig(7a): Mean Doppler profile of 24 July 2002 using FFT



Fig(7b): Mean Doppler profile of 24 July 2002 using HHT



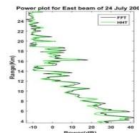
Fig(7c): Doppler plot extracted from Fig (7a)



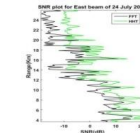
Fig(7d): Doppler plot extracted from Fig (7b)

176
177

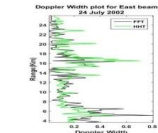
178



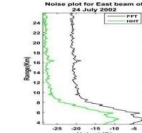
Fig(7e): Power plot for East beam of 24 July 2002



Fig(7f): SNR plot for East beam of 24 July 2002



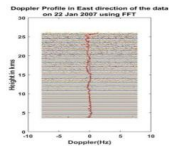
Fig(7g): Doppler width for East beam of 24 July 2002



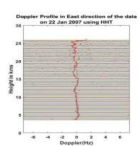
Fig(7h): Noise plot for East beam of 24 July 2002

179
180
181

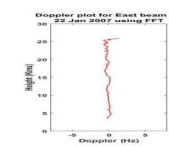
182



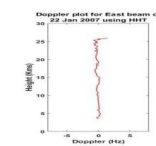
Fig(8a): Mean Doppler profile using FFT of 22 Jan 2007



Fig(8b): Mean Doppler profile using HHT of 22 Jan 2007



Fig(8c): Doppler plot extracted from Fig (8a)



Fig(8d): Doppler plot extracted from Fig (8b)

183
184

185

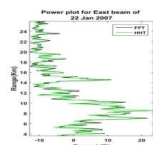
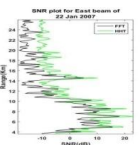
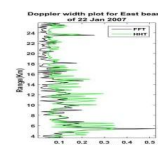


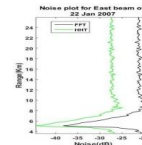
Fig (8e): Power plot for East beam of 22 Jan 2007



Fig(8f): SNR plot for East beam of 22 Jan 2007



Fig(8g): Doppler width for East beam of 22 Jan 2007



Fig(8h): Noise plot for East beam of 22 Jan 2007

186
187
188
189

Table1 : Average values of SNR, Power and Noise for Each beam of two different data sets

Beam	24 July 2002				22 Jan 2007							
	SNR (dB)		Power(dB)		SNR(dB)		Power(dB)		Noise(dB)			
	FFT	HHT	FFT	HHT	FFT	HHT	FFT	HHT	FFT	HHT		
East	-3.9000	1.8708	5.3278	4.2719	-17.8649	-24.0106	-2.8712	2.1041	5.1030	4.2651	-18.6521	-25.1496
West	-3.8707	2.0951	5.0638	4.0296	-18.1582	-24.0236	-2.0108	2.3162	4.9824	3.8526	-18.2195	-24.8815
Z-Y	-2.0122	3.9113	6.3488	6.2723	-18.7317	-25.4112	1.1265	5.1198	5.8962	5.0357	-19.1154	-25.0163
Z-X	1.0270	7.1109	8.4686	7.9878	-19.6510	-26.2158	1.5381	6.2547	7.5149	6.1491	-18.3125	-24.9167
North	-1.4652	3.7248	6.1634	5.3566	-19.4641	-25.4609	-1.3284	3.0010	5.9632	5.1026	-19.7732	-25.8064
South	-0.7526	4.2647	6.6162	5.6437	-19.7239	-25.7137	-1.0631	3.9962	6.1173	5.9427	-19.8451	-24.5331

190
191



192 **Table 2: Average values of SNR, Power and Noise for all the beams**

24 July 2002						22 Jan 2007					
SNR(dB)		Power(dB)		Noise(dB)		SNR(dB)		Power(dB)		Noise(dB)	
FFT	HHT	FFT	HHT	FFT	HHT	FFT	HHT	FFT	HHT	FFT	HHT
-1.8289	3.8296	6.3314	5.5936	-18.9323	-25.1393	-0.7681	3.7986	5.9295	5.0579	-18.9863	-25.0506

193 **7. Conclusion**

194 Thus an efficient algorithm based on Empirical Mode Decomposition de-noising using soft threshold technique
 195 for accurate doppler profile detection and improved SNR for MST Radar Signals was developed. Further,
 196 spectral moments were estimated and signal parameters such as mean doppler, signal power, noise power and
 197 SNR were calculated and the algorithm was tested on different radar data sets for its efficacy in comparison to
 198 FFT. It has been observed that there is a considerable improvement in recognition of the doppler echo and SNR.

199 **Acknowledgements**

200 This research work is supported by the Indian Space Research Organization (ISRO under RESPOND scheme)
 201 #B.19012/72/2014-II,12/11/2014. We thank National Atmospheric Research Laboratory (NARL), Gadanki for
 202 providing the MST Radar data and appreciate helpful comments from the Scientists, NARL.

203 **References**

- 204 Hildebrand, P.H., and Sekhon, R.S.: "Objective determination of the noise level in Doppler spectra," J.Appl.
 205 Meteorol. 13, pp 808-811, 1974.
 206 Woodman, R.F., "Spectral moments estimation in MST radars," Radio Science., Vol. 20, pp 1185-1195, 1985.
 207 Morse, C. S., Goodrich, R.K. and Cornman, L.B.: "The NIMA method for improved moment estimation
 208 from Doppler spectra," J. Atmos. Oceanic Technol., 19, 274–295,2002.
 209 Anandan,V.K., Balamuralidhar, P., Rao, P.B., Jain, A. R. and Pan, C. J.: "An Adaptive Moments Estimation
 210 Technique Applied to MST Radar Echoes," Journal of Atmospheric and Oceanic Technology, Volume
 211 22.2004
 212 Padmaja, N., Varadarajan, S. and Swathi, R.: "Signal Processing of Radar echoes using Wavelets and Hilbert
 213 Huang Transform," Signal & Image Processing: An International Journal (SIPIJ) Vol.2, No.3, September
 214 2011
 215 Jing-tian, T., Qing, Z., Yan, T., Bin, L. and Xiao-kai, Z.: "Hilbert Huang Transform for ECG de-noising," 1st
 216 International Conference on Bioinformatics and Biomedical Engineering, 2007.
 217 Huang, N.E. and Wu, Z.: "Statistical significance test of intrinsic mode functions," Hilbert-Huang
 218 Transform and Its
 219 Applications, World Scientific Publishing Company, first edition, 2005.
 220 George solis, T. and Thomas Xenos,D.: "Signal Denoising Using Empirical Mode Decomposition and Higher
 221 Order Statistics," International Journal of Signal Processing, Image Processing and Pattern Recognition Vol.
 222 4, No. 2, June, 2011.
 223 Flandrin,P., Rilling,G. and Goncalves, P.: "Empirical mode decomposition as a filter bank," IEEE Signal
 224 Processing Lett., vol. 11, pp. 112–114, Feb. 2004.
 225 Norden Huang, E., Shen, Z. Long, S.R., Wu, M.L., Shih, E.H., Zheng, Q., Tung, C.C. and Liu, H.H.: "The
 226 Empirical Mode Decomposition and the Hilbert Spectrum for Nonlinear and Non-stationary Time Series
 227 Analysis," Proceedings of the Royal Society of London, Vol. 454, pp 903–995, 1998.
 228 Wu Z. and Huang, N. E.: "A study of the characteristics of white noise using the empirical mode decomposition
 229 method," Proc. Roy. Soc London A, 460, 1597–1611,2004.
 230 Dejie Yu, Junsheng Cheng and Yu Yang, "Empirical Mode Decomposition for Trivariate Signals," IEEE
 231 Transactions on Signal processing, Volume: 58, Issue: 3, pp.1059-1068 March 2010
 232 Rilling, G., Flandrin, P. and Goncalves, P.: "On empirical mode decomposition and its algorithms," Proc. IEEE-
 233 EURASIP Workshop on Nonlinear Signal and Image Processing, June 2003.
 234 Flandrin, P., Gonçaves, P. and Rilling, G. "Detrending and denoising with Empirical Mode
 235 Decompositions", Proceedings of Eusipco, Wien (Austria), pp. 1581-1584, September 2004.
 236 Padmaja, N., Varadarajan,S. and Ramykrishna, E.: "EMD denoising of MST Radar echoes using Soft
 237 thresholding", Third URSI Regional Conference on Radio Science March 2017, NARL, Tirupati.
 238 Donoho D. L.: "Denoising by Soft Thresholding", IEEE transactions on Information Theory, Vol. 41, pp.613-
 239 627, 1995.
 240